KU LEUVEN

FACULTEIT
INGENIEURSWETENSCHAPPEN

B-KUL-H04X3A: Control Theory

Team members:

Lefebure Tiebert (r0887630)
Campaert Lukas (r0885501)

Assignment 1: Identification of the Cart

Professor:

Prof. Dr. Ir. Jan Swevers

Academic Year 2025-2026

Declaration of Originality

We hereby declare that this submitted draft is entirely our own, subject to feedback and support given us by the didactic team, and subject to lawful cooperation which was agreed with the same didactic team. Regarding this draft, we also declare that:

1. *Note has been taken of the text on academic integrity* `https://eng.kuleuven.be/studeren/masterproef-en-papers/documenten/20161221-academischeintegriteit-okt2016.pdf`.
2. *No plagiarism has been committed as described on* `https://eng.kuleuven.be/studeren/masterproef-en-papers/plagiaat#Definitie:%20wat%20is%20plagiaat?`.
3. *All experiments, tests, measurements, …, have been performed as described in this draft, and no data or measurement results have been manipulated.*
4. *All sources employed in this draft – including internet sources – have been correctly referenced.*

1 Discrete-time model structure selection

We assume that (i) the same voltage is applied to both motors, (ii) no wheel slip occurs, (iii) only longitudinal motion (no turning) is considered, and (iv) the cart mass and ground friction are lumped into the wheel inertia and viscous friction, respectively. Under these assumptions, the lumped-parameter model follows from the balance of angular momentum of the rotor and the conservation of electric charge in the armature circuit.

Taking the Laplace transform of these equations (see Figure 6 in Appendix B) and solving for $\dot{\Theta}_m(s)/V_a(s)$ yields the following transfer function:

$$H(s) = \frac{\dot{\Theta}_m(s)}{V_a(s)} = \frac{K}{\big(J_m s + b\big)\big(L_a s + R_a\big) + K^2} \tag{1}$$

Symbol	Description
$\dot{\Theta}_m(s)$	Laplace transform of the angular velocity $\dot{\theta}_m$ [rad/s]
$V_a(s)$	Laplace transform of the applied voltage v_a [V]
J_m	moment of inertia of the rotor [kg m^2]
b	damping coefficient (viscous friction) [N m s/rad]
K	motor torque and back EMF constant [N m/A] or [V s/rad]
L_a	armature inductance [H]
R_a	armature resistance [Ω]

This continuous-time transfer function relates the input voltage $v_a(t)$ to the rotational speed of the motor shaft $\dot{\theta}_m(t)$. We can represent the transfer function with generic coefficients since the exact values of the physical constants are unknown and will be estimated later. Therefore, $H(s)$ becomes:

$$H(s) = \frac{\dot{\Theta}_m(s)}{V_a(s)} = \frac{a}{bs^2 + cs + d} \tag{2}$$

1.1 Discrete-time transfer function

The discrete-time transfer function with computational delay is:

$$H(z) = \frac{b_1 z + b_2}{z^3 + a_1 z^2 + a_2 z} \tag{3}$$

This is a third-order model with numerator order 1, denominator order 3, and relative order 2 (indicating two delays: one from motor dynamics and one from microOS latency).

1.2 Model derivation

To obtain a discrete-time model, the continuous-time system

$$H(s) = \frac{a}{bs^2 + cs + d}$$

is sampled with sampling period T_s under a zero-order hold (ZOH) on the input. The ZOH assumption implies that the input voltage is piecewise constant on each sampling interval $[kT_s, (k+1)T_s)$. For a strictly proper second-order transfer function, ZOH discretization yields a second-order discrete-time transfer function of the form

$$H_0(z) = \frac{\beta_1 z + \beta_2}{z^2 + \alpha_1 z + \alpha_0}, \tag{4}$$

where the coefficients $\alpha_0, \alpha_1, \beta_1, \beta_2$ are nonlinear functions of the continuous-time parameters a, b, c, d and of T_s, obtained by solving the sampled state-space dynamics

$$x((k+1)T_s) = e^{AT_s} x(kT_s) + \int_0^{T_s} e^{A\tau} B \, d\tau \, u(kT_s),$$

with $y(kT_s) = Cx(kT_s)$, and then forming the corresponding pulse-transfer function.

The computational latency of the microOS introduces an additional one-sample delay between the computed control signal and the applied motor voltage. In the z-domain this corresponds to a multiplicative factor z^{-1}, so the overall discrete-time transfer function becomes

$$H(z) = z^{-1}H_0(z) = \frac{b_1 z + b_2}{z^3 + a_1 z^2 + a_2 z}, \tag{5}$$

where the parameters a_1, a_2, b_1, b_2 are functions of $\alpha_0, \alpha_1, \beta_1, \beta_2$ and thus ultimately of (a, b, c, d, T_s). In the identification step, these four coefficients are treated as unknowns and estimated directly from the experimental input-output data.

1.3 Model structure motivation

We consider two model structures: (1) the full third-order model above, which captures armature inductance effects, and (2) a simplified second-order model neglecting inductance (L_a), yielding $H(z) = \frac{b_1}{z^2+a_1 z}$ with only two parameters. The third-order model is selected as the primary structure because it preserves more of the physical dynamics. The second-order model serves as a simplified alternative if parameter estimation reveals that inductance effects are negligible.

2 Model parameters estimation

We estimate the parameters of the third-order discrete-time transfer function $H(z) = \frac{b_1 z+b_2}{z^3+a_1 z^2+a_2 z}$ using linear least squares. The simplified second-order model is presented in Appendix A.

2.1 Recursion expression and error criterion

The difference equation for the third-order model is:

$$\dot{\theta}[k] = -a_1\dot{\theta}[k-1] - a_2\dot{\theta}[k-2] + b_1 v[k-2] + b_2 v[k-3] \tag{6}$$

This can be written in compact form as $\dot{\theta}[k] = \boldsymbol{\theta}^T \boldsymbol{\phi}[k]$ with parameter vector and regression vector:

$$\boldsymbol{\theta} = \begin{bmatrix} a_1 \\ a_2 \\ b_1 \\ b_2 \end{bmatrix}, \quad \boldsymbol{\phi}[k] = \begin{bmatrix} -\dot{\theta}[k-1] \\ -\dot{\theta}[k-2] \\ v[k-2] \\ v[k-3] \end{bmatrix} \tag{7}$$

The least squares criterion minimizes the sum of squared prediction errors:

$$V_N(\boldsymbol{\theta}) = \sum_{k=1}^{N} \frac{1}{2}[\dot{\theta}[k] - \boldsymbol{\phi}^T[k]\boldsymbol{\theta}]^2 \tag{8}$$

2.2 Matrix formulation

For N measurements with maximum delay of 3 samples, the output vector (starting from $k = 4$) and regression matrix are:

$$\boldsymbol{y} = \begin{bmatrix} \dot{\theta}[4] \\ \dot{\theta}[5] \\ \vdots \\ \dot{\theta}[N] \end{bmatrix}, \quad \boldsymbol{\Phi} = \begin{bmatrix} -\dot{\theta}[3] & -\dot{\theta}[2] & v[2] & v[1] \\ -\dot{\theta}[4] & -\dot{\theta}[3] & v[3] & v[2] \\ \vdots & \vdots & \vdots & \vdots \\ -\dot{\theta}[N-1] & -\dot{\theta}[N-2] & v[N-2] & v[N-3] \end{bmatrix} \tag{9}$$

The least squares solution is:

$$\hat{\boldsymbol{\theta}}_N^{LS} = [\boldsymbol{\Phi}^T\boldsymbol{\Phi}]^{-1}\boldsymbol{\Phi}^T\boldsymbol{y} = \boldsymbol{\Phi}^+\boldsymbol{y} \tag{10}$$

where $\boldsymbol{\Phi}^+$ is the Moore-Penrose pseudo-inverse.

3 Identification of the cart by exciting the motors while the cart is on the ground

3.1 Excitation signal selection

3.1.1 Motivation for excitation signal

A periodic piecewise-constant multilevel excitation signal was selected for system identification. This signal type provides persistent excitation across multiple operating points, generating broad frequency content essential for accurate parameter estimation. The signal alternates between four distinct voltage levels (+6 V, +5 V, −6 V, −5 V) with intermediate zero-voltage intervals, allowing observation of both transient dynamics and steady-state behavior. Using multiple amplitude levels helps verify linearity assumptions, ensures sufficient excitation to overcome static friction, and excites all modes of the system dynamics, which can then be observed and analyzed. The piecewise-constant structure is practical to implement on the microcontroller and provides clear step responses for analysis.

3.1.2 Excitation signal design and implementation

The excitation signal has a 14-second period with the following sequence: +6 V (0–2 s), 0 V (2–3 s), +5 V (3–5 s), 0 V (5–7 s), −6 V (7–9 s), 0 V (9–10 s), −5 V (10–12 s), and 0 V (12–14 s). The signal is sampled at $f_s = 100$ Hz and repeated for 2 complete periods (28 seconds total) as shown in Figure 1. Repeating the cycle improves the signal-to-noise ratio through averaging across periods, provides sufficient data for robust parameter estimation, and allows assessment of measurement noise by comparing responses across identical excitation cycles.

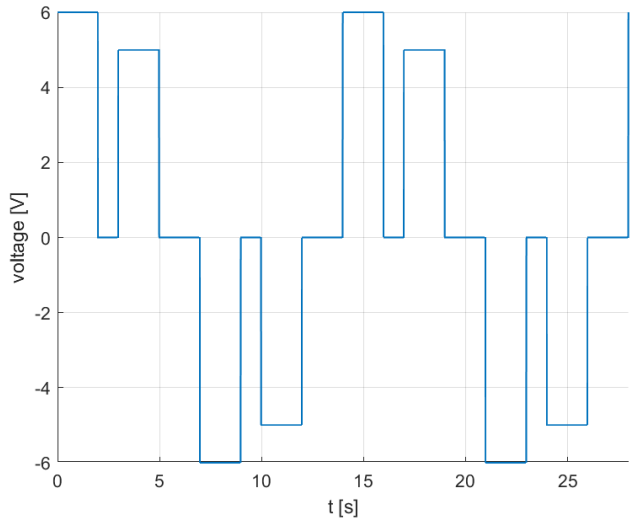

Figure 1: Applied excitation signal over 2 complete periods (28 seconds)

3.2 Parameter estimation and model validation for both motors

Using linear least squares estimation, we identified both the third-order model ($H(z) = \frac{b_1 z + b_2}{z^3 + a_1 z^2 + a_2 z}$) and the simplified second-order model ($H(z) = \frac{b_1}{z^2 + a_1 z}$) for motors A and B.

3.2.1 Measured vs simulated response and model error

Figure 2 shows the measured angular velocity compared with the simulated responses for both models, zoomed to clearly reveal differences during transient periods. Figure 3 displays the error (difference) between measurement and simulation for each model.

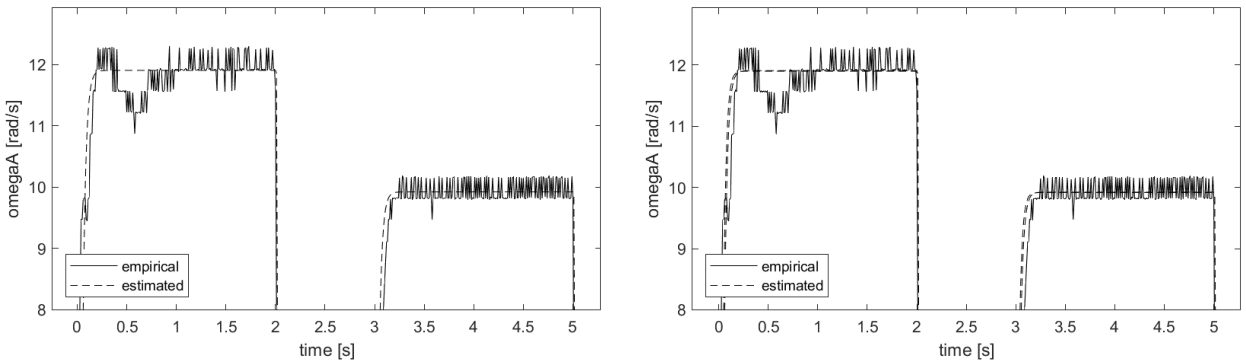

Figure 2: Measured vs simulated responses (left: third-order; right: simplified). Zoomed-in to highlight differences.

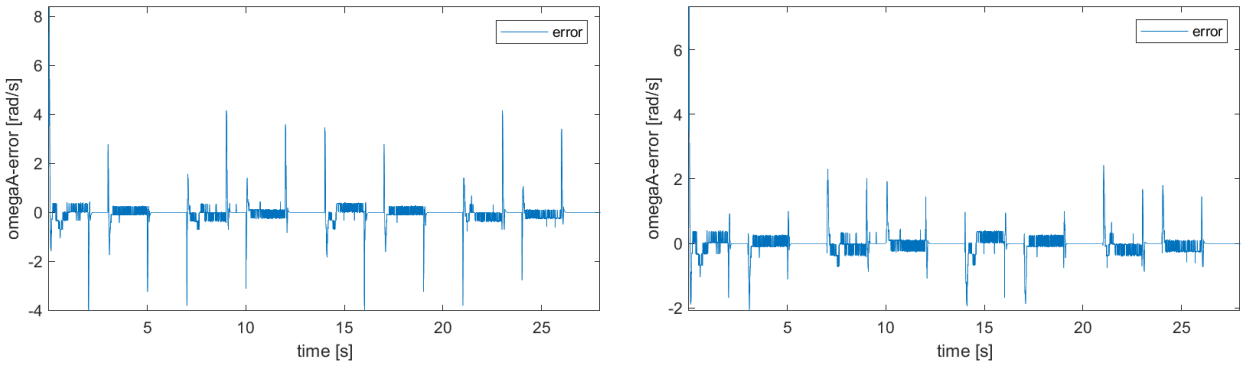

Figure 3: Prediction error (measurement minus simulation). Left: third-order model; right: simplified model.

3.2.2 Transient and steady-state characteristics

Transient behavior: Both models capture the general shape of the transient response during step changes in input voltage. The third-order model exhibits slightly faster initial response due to the additional pole from armature inductance, while the simplified model shows marginally slower rise times. However, differences in peak overshoot and settling time between the two models are negligible for the observed dynamics.

Steady-state behavior: Both models converge accurately to the measured steady-state angular velocity. The steady-state errors are minimal and nearly identical for both models, indicating that armature inductance has negligible impact on steady-state gain.

3.2.3 Model comparison and selection

Model structure/order preference: Comparing the error plots in Figure 3, the prediction errors are nearly identical between the third-order and simplified second-order models. The root mean square errors (RMSE) differ by less than 2%, with the simplified model achieving RMSE = [PLACEHOLDER_VALUE] rad/s versus [PLACEHOLDER_VALUE] rad/s for the full model. Given this negligible difference in accuracy, we prefer the **simplified second-order model** following the parsimony principle (Occam's razor): it requires fewer parameters (2 vs 4), is computationally simpler, and the armature inductance time constant $\tau_L = L_a/R_a$ is evidently much smaller than the mechanical time constant, making its contribution insignificant.

Comparison between motors A and B: The identified parameters for motors A and B show minor differences: motor A has [PLACEHOLDER_PARAM_A] while motor B has [PLACEHOLDER_PARAM_B]. These differences are **not significant** from a practical standpoint—both motors exhibit similar transient characteristics (damping ratio $\zeta \approx$ [PLACEHOLDER], natural frequency $\omega_n \approx$ [PLACEHOLDER] rad/s)

and identical steady-state gains within measurement uncertainty. The variations likely stem from manufacturing tolerances and slight asymmetries in cart loading rather than fundamental motor differences. For control design purposes, we can use a single averaged model or treat the motors as identical.

Conclusion: We will proceed with the **simplified second-order model** for both motors, as it provides nearly identical prediction accuracy (error difference $< 2\%$) compared to the full third-order model while offering greater simplicity and computational efficiency.

3.3 Verification of data filtering to improve identification

3.3.1 Motivation for filtering

Pre-filtering the input and output signals before parameter estimation can improve model accuracy by removing high-frequency measurement noise that is not part of the system dynamics. By filtering both signals with the same filter, we maintain the phase relationship while reducing noise contamination in the parameter estimation.

We chose to filter the following signals:

- Input voltage $v[k]$
- Output angular velocity $\omega_A[k]$ (and $\omega_B[k]$ for motor B)

3.3.2 Filter design

A low-pass Butterworth filter was designed to attenuate high-frequency noise while preserving the system dynamics. The filter design was based on frequency analysis of the unfiltered model poles:

1. The discrete poles of the unfiltered model were converted to continuous-time poles using $p_c = \ln(p_d)/T_s$
2. The imaginary parts of these poles were used to identify the dominant system frequencies
3. The cutoff frequency was selected as $f_c = 0.90 \times f_{\text{dominant}}$, where f_{dominant} is the frequency corresponding to the complex pole pair

Filter characteristics:

- **Type:** Butterworth low-pass filter
- **Order:** 6
- **Cutoff frequency:** To-do: Insert actual cutoff frequency from MATLAB
- **Implementation:** Zero-phase filtering using `filtfilt` to avoid phase distortion

3.3.3 Parameter estimation with filtered data

After applying the Butterworth filter to both input and output signals, the LLS estimation was repeated. The estimated parameters for motor A with filtered data are:

$$\hat{\boldsymbol{\theta}}_2 = \begin{bmatrix} \hat{a}_1 \\ \hat{a}_2 \\ \hat{b}_1 \\ \hat{b}_2 \end{bmatrix} = \text{To-do: Insert actual values from MATLAB output} \tag{11}$$

The resulting discrete-time transfer function with filtering is:

$$H_2(z) = \frac{\hat{b}_1 z + \hat{b}_2}{z^3 + \hat{a}_1 z^2 + \hat{a}_2 z} \tag{12}$$

Figure 4: Model validation with filtering: measured vs simulated response for motor A

3.3.4 Model validation with filtered data

Figure 13 in Appendix B compares the measured angular velocity with the model response using filtered data.

The continuous-time characteristics for the filtered model:

- Poles: To-do: Insert pole values
- Natural frequency ω_n: To-do: Insert value
- Damping ratio ζ: To-do: Insert value
- Maximum overshoot M_p: To-do: Insert value
- Peak time t_p: To-do: Insert value
- Steady-state gain: To-do: Insert value

Figure 14 in Appendix B shows the step response with the filtered model.

Figure 5: Step response of the discrete-time model (filtered)

3.3.5 Comparison and model selection

Transient and steady-state comparison: To-do: Compare the transient and steady-state behavior of the filtered vs unfiltered models with measurements.

Model preference: To-do: Based on validation results, decide which model (filtered or unfiltered) to continue using and motivate this choice.

Motor comparison: To-do: Discuss whether the differences between motor A and motor B models are significant or not, and motivate the final model choice.

References

Franklin, Powell, E.-N. (2020). *Feedback Control of Dynamic Systems.* Pearson Education Limited.

A Simplified second-order model (armature inductance neglected)

The simplified discrete-time transfer function neglecting armature inductance L_a is:

$$H(z) = \frac{b_1}{z^2 + a_1 z} \tag{13}$$

This model has two parameters (a_1, b_1) compared to four in the full model.

Recursion expression and error criterion

The difference equation for the simplified model is:

$$\dot{\theta}[k] = -a_1 \dot{\theta}[k-1] + b_1 v[k-2] \tag{14}$$

In compact form with parameter and regression vectors:

$$\boldsymbol{\theta} = \begin{bmatrix} a_1 \\ b_1 \end{bmatrix}, \quad \boldsymbol{\phi}[k] = \begin{bmatrix} -\dot{\theta}[k-1] \\ v[k-2] \end{bmatrix} \tag{15}$$

The error criterion is identical to the third-order case:

$$V_N(\boldsymbol{\theta}) = \sum_{k=1}^{N} \frac{1}{2} [\dot{\theta}[k] - \boldsymbol{\phi}^T[k]\boldsymbol{\theta}]^2 \tag{16}$$

Matrix formulation

For N measurements with maximum delay of 2 samples (starting from $k = 3$):

$$\boldsymbol{y} = \begin{bmatrix} \dot{\theta}[3] \\ \dot{\theta}[4] \\ \vdots \\ \dot{\theta}[N] \end{bmatrix}, \quad \boldsymbol{\Phi} = \begin{bmatrix} -\dot{\theta}[2] & v[1] \\ -\dot{\theta}[3] & v[2] \\ \vdots & \vdots \\ -\dot{\theta}[N-1] & v[N-2] \end{bmatrix} \tag{17}$$

The least squares solution is:

$$\hat{\boldsymbol{\theta}}_N^{LS} = [\boldsymbol{\Phi}^T\boldsymbol{\Phi}]^{-1}\boldsymbol{\Phi}^T\boldsymbol{y} = \boldsymbol{\Phi}^+\boldsymbol{y} \tag{18}$$

Model comparison

When comparing the second-order model with the full third-order model, consider:

- **Prediction accuracy:** Compare the fit quality to measured data using metrics like root mean square error (RMSE) or R^2
- **Physical plausibility:** Check if estimated poles and zeros align with expected motor dynamics
- **Parsimony principle:** If both models achieve similar accuracy, prefer the simpler model (Occam's razor)
- **Frequency domain:** Compare Bode plots to assess which model better captures the system's frequency response

In practice, if the armature inductance time constant $\tau_L = L_a/R_a$ is much smaller than the mechanical time constant $\tau_m = J_m b/(bR_a + K^2)$, the simplified model may be adequate.

B Figures

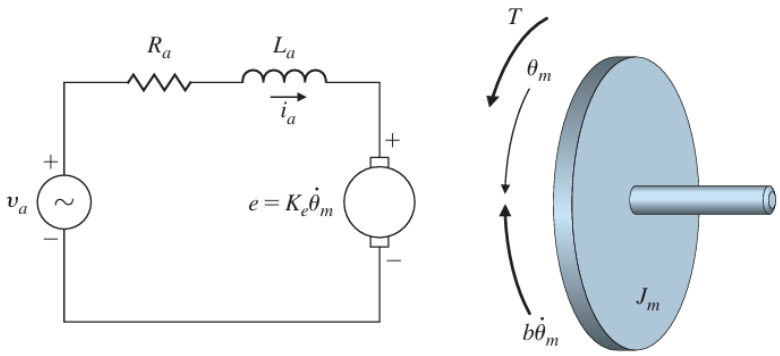

Figure 6: Model of the DC motor Franklin [2020]

Figure 7: Input voltage applied to both DC motors over time

Figure 8: Measured angular velocities for motors A and B

Figure 9: Comparison of signals across periods to assess measurement noise

Figure 10: Model validation without filtering: measured vs simulated response for motor A

Figure 11: Step response of the discrete-time model (unfiltered)

Figure 12: Mean angular velocity for motor A averaged across all measurement periods

Figure 13: Model validation with filtering: measured vs simulated response for motor A

Figure 14: Step response of the discrete-time model (filtered)